JOURNAL OF MAGNETIC RESONANCE **128,** 217–227 (1997)
ARTICLE NO. MN971222

Determination of Orientational Anisotropy in Glassy Solids by 2D Dipolar Spectra With Sample Flipping

Marcel Utz,*,† J. Eisenegger,* Ulrich W. Suter,† and Richard R. Ernst*

*Laboratorium für physikalische Chemie und †Departement Werkstoffe, Institut für Polymere, Eidgenössische Technische Hochschule, CH-8092 Zürich, Switzerland

Received March 25, 1997; revised July 21, 1997

A method is proposed for the quantitative measurement of orientational anisotropy in glassy solids based on 2D dipolar NMR spectra with sample flipping (dipolar DECODER experiment). Purely dipolar spectra are obtained by chemical shift refocusing by a multiple pulse sequence. The experiment is applied to an investigation of a doubly ^{13}C-labeled sample of bisphenol-A polycarbonate deformed in a channel-die apparatus. The orientational distribution function is determined by an expansion of the distribution in terms of spherical harmonics up to degree four. © 1997 Academic Press

INTRODUCTION

Solid polymers used in technical applications are mostly anisotropic. All commercially important techniques to shape raw polymer granulate into a final form, such as extrusion, fiber drawing, or injection molding, lead to a partial segmental orientation of the polymer chains. The resulting anisotropy can have a profound impact on the mechanical properties of the product (*1*). For this reason, the quantification of the orientational order in polymers and other glassy solids has received much scientific attention.

Several spectroscopic measurements are sensitive to orientational order. For instance, infrared dichroism spectra are susceptible to the orientational distribution of the transition dipoles associated with a particular line in the spectrum (*2*). The vibrational modes that are observed in the IR spectrum usually extend over several atoms and can also be influenced by the intermolecular packing in a glassy solid. Thus, the identification of a spectral line with a well-defined molecular director is often difficult (*2*). Moreover, insufficient spectral resolution of inequivalent groups can obscure the orientational information.

X-ray and neutron scattering have been used extensively to measure the preferential orientation of crystallites in semicrystalline polymers (*3, 4*). However, in amorphous solids, where long-range translational order is absent, segmental orientation is more difficult to quantify from scattering data (*5*).

Solid-state NMR spectroscopy has been shown to be a powerful tool for the quantification of orientational order in amorphous as well as semicrystalline polymers (*6–11*). Information on the orientational distribution function can be obtained from the anisotropic interaction tensors contained in the spin Hamiltonian. They comprise the chemical shielding tensor, the quadrupolar coupling tensor, and the dipolar coupling tensor. Among those, the first two have so far been applied for investigating orientational order in anisotropic polymer samples (*6–11*).

For the unambiguous orientation of a rigid molecular fragment, in general, three Euler angles are needed while a one-dimensional NMR experiment delivers for each interaction tensor just a single observable frequency, insufficient to determine the full orientation or its distribution function. Sometimes it is possible to take advantage of several tensor interactions, rigidly related to the same molecular fragment. Then more orientational information is available, although its evaluation in the case of an angular distribution might be ambigous. A somewhat related problem lies in the fact that the NMR experiment is axially symmetric around the direction of the static magnetic field. Without further precautions, only the uniaxial average of the orientational distribution function can be derived from NMR spectra, irrespective of the pulse sequence.

To handle this situation, Henrichs (*6*) proposed a clever two- or three-dimensional experiment where between the detection and the different evolution periods the sample is rapidly reoriented. This breaks the uniaxial symmetry of the NMR experiment and allows one to measure two or three frequencies associated with each interaction tensor, from which a unique orientation of the tensor and its full distribution function can be determined. Later, Schmidt-Rohr *et al.* coined the acronym DECODER for this experiment (*8, 9*). It has so far been applied to CSA tensor (*8, 9*) and quadrupolar tensor (*8*) measurements. We refer to these two applications as CSA–DECODER and quadrupolar DECODER experiments.

In this contribution, we apply the DECODER principle to

1090-7807/97 $25.00

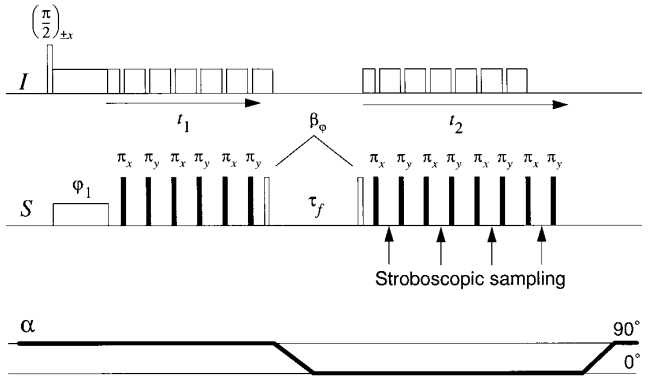

FIG. 1. The dipolar DECODER pulse sequence. The chemical shift term is suppressed both during the evolution and the detection periods by a xy-4 sequence. During the time delay τ_f, the orientation of the sample is changed. The selection of the pulse rotation angle β is specified in the text.

measure the orientational distribution function of the dipolar coupling tensor in doubly ^{13}C-labeled polymers. A modified pulse sequence, shown in Fig. 1, is introduced which suppresses chemical shift effects. We call this experiment ''dipolar DECODER''.

The principal advantage of using the dipolar tensor for orientation studies is the fact that the dipolar interaction is uniquely related to an internuclear vector and is free from any perturbing neighbor effects in contrast to the CSA and quadrupolar interactions, which are governed by electronic terms that reflect the molecular environment and are not related in a simple, predictable manner to the molecular frame. The dipolar interaction allows one to measure accurate internuclear distances and the orientation of internuclear vectors, provided that the molecular fragment is immobile.

The uniaxial character of the dipolar interaction allows for a complete description of its orientation by two polar angles. This leads to simpler 2D spectra and facilitates the calculation of orientation distribution functions from the spectral data (*8*). Obviously, the information content is thereby reduced in comparison to the full orientational distribution function of an asymmetric tensor.

With specifically pairwise isotopically enriched samples it is possible to select the direction of the reference axis according to the question in mind. This could be of importance for applications where the orientation of a particular side chain plays a major role, for example, in side-chain liquid crystalline polymers or in organic semiconductors.

In the present study, the dipolar DECODER technique will be applied to the investigation of plastic deformation of glassy bisphenol-A polycarbonate. A solid sample is plastically deformed in plane-strain mode using a channel die. The resulting molecular orientational anisotropy is investigated based on the dipolar interaction between two specifically ^{13}C-labeled sites in the polymer chain.

THE DIPOLAR DECODER EXPERIMENT

The dipolar DECODER experiment, shown in Fig. 1, starts with a standard Hartmann–Hahn cross-polarization period for polarizing the *S* (^{13}C) spins. It is followed by an evolution period during which *I*-spin (proton) decoupling is applied and the effects of *S*-spin chemical shifts are refocused. After storage of selected coherence components in the form of polarization by a pulse of rotation angle β and phase φ, the sample is flipped by the angle α about an axis perpendicular to the static magnetic field. A further β_φ pulse starts the precession for the detection period that proceeds again under *I*-spin decoupling and repetitive chemical shift refocusing. The sampling process is stroboscopically synchronized with the pulse sequence for chemical shift refocusing. The proper selection of the refocusing pulse sequence proved to be essential for the success of the experiment and will be discussed below. The resulting 2D spectrum is treated by standard 2D data processing procedures, except for a specific phase-cycling procedure for the coherence-transfer selection to be discussed in the following.

Phase Cycle for Exclusive DECODER Spectroscopy

The symmetry of the dipolar Pake doublet with two transition frequencies for each orientation leads for a straight 2D dipolar DECODER experiment to a quadratic pattern with fourfold redundancy and numerous overlapping features. This renders its analysis more difficult and calls for procedures of simplification. In particular, the mixing between within the pairs of transitions should be inhibited by a proper selection of the coherence transfer pathways. This task has some similarity with exclusive correlation spectroscopy (E.COSY) (*12*), and we call the resulting procedure exclusive dipolar DECODER or E.DECODER. It is related to deuterium 2D exchange spectroscopy (*13*) as two spins $\frac{1}{2}$ under a purely dipolar Hamiltonian behave like a pseudo spin 1.

The proper phase cycle can be found by computing the response of two spins $\frac{1}{2}$ with a purely dipolar Hamiltonian

$$H_d = b_{12}(\Theta_{12})\{2S_{1z}S_{2z} - \tfrac{1}{2}(S_1^+S_2^- + S_1^-S_2^+)\} \qquad [1]$$

with

$$b_{12}(\Theta_{12}) = -\frac{\mu_0}{4\pi}\frac{\gamma_s^2\hbar}{r_{12}^3}\frac{1}{2}(3\cos^2\Theta_{12} - 1), \qquad [2]$$

and the angle Θ_{12} between the internuclear vector and the magnetic field direction. The density operator after the cross-polarization process of the dipolar DECODER experiment contains the relevant term $\sigma(0) = S_{1x} + S_{2x}$. It can be decomposed into two coherences

$$\sigma(0) = C^p + C^n, \qquad [3]$$

with

$$C^p = \tfrac{1}{2}(S_1^\alpha S_2^+ + S_1^+ S_2^\alpha) + \tfrac{1}{2}(S_1^\beta S_2^- + S_1^- S_2^\beta) \qquad [4]$$

$$C^n = \tfrac{1}{2}(S_1^\alpha S_2^- + S_1^- S_2^\alpha) + \tfrac{1}{2}(S_1^\beta S_2^+ + S_1^+ S_2^\beta), \qquad [5]$$

where $S_i^\alpha = \tfrac{1}{2}1_i + S_{iz}$ and $S_i^\beta = \tfrac{1}{2}1_i - S_{iz}$.

Under H_d, the two coherences C^p and C^n precess with the frequencies $\pm\Omega_1 = \pm\frac{3}{2}b_{12}(\Theta_{12}^{(1)})$, respectively, leading to

$$\sigma(t_1) = C^p \exp(i\Omega_1 t_1) + C^n \exp(-i\Omega_1 t_1). \qquad [6]$$

Before the sample is flipped to a new position with the angle $\Theta_{12}^{(2)}$, the coherence is converted into either Zeeman order or dipolar order with a $(\pi/2)_x$ pulse or a $(\pi/4)_y$ pulse, respectively. The same pulse is needed after the sample flip for the recovery of coherence. It evolves during the detection period as

$$\sigma_{ZO}(t_1, t_2) = \tfrac{1}{2}[\cos\Omega_1 t_1 \exp(i\Omega_2 t_2) C^p + \cos\Omega_1 t_1 \exp(-i\Omega_2 t_2) C^n] \qquad [7]$$

and

$$\sigma_{DO}(t_1, t_2) = \tfrac{1}{4}[\sin\Omega_1 t_1 \exp(i\Omega_2 t_2) C^p - \sin\Omega_1 t_1 \exp(-i\Omega_2 t_2) C^n], \qquad [8]$$

depending on the selection of Zeeman or dipolar order. Here, $\Omega_2 = \frac{3}{2}b_{12}(\Theta_{12}^{(2)})$. The terms from Eqs. [7] and [8] produce four peaks at the positions $(\pm\Omega_1, \pm\Omega_2)$. On the other hand, for the combination

$$\sigma_{ZO}(t_1, t_2) + 2i\sigma_{DO}(t_1, t_2) = \tfrac{1}{2}[\exp(i\Omega_1 t_1)\exp(i\Omega_2 t_2) C^p + \exp(-i\Omega_1 t_1)\exp(-i\Omega_2 t_2) C^n] \qquad [9]$$

only the two peaks at (Ω_1, Ω_2) and $(-\Omega_1, -\Omega_2)$ remain, leading as desired to a simplified peak pattern with C_2 symmetry.

The exclusive dipolar DECODER experiment thus consists of recording two sets of signals for the mixing pulses $(\pi/2)_y$ and $(\pi/4)_x$, multiplying the second by a factor $2i$, and adding the two sets.

Generation of a Purely Dipolar Hamiltonian

As has been outlined above, it is of advantage to suppress the chemical shift term in the Hamiltonian in order to selectively retrieve information from the dipolar coupling tensor. During the evolution period, chemical shift refocusing is quite easily achieved by the application of a central π pulse (*14*). It is well known that this kind of refocusing works only for weakly coupled spin systems (*15*). In the present situation where strong dipolar coupling cannot be avoided, the chemical shift difference remains in the expression for the transition frequencies, and a more refined simulation procedure is necessary to compute the resulting peak shapes (*14–17*).

For the dipolar DECODER experiment, shift refocusing is required also during the detection period and necessitates a repetitive refocusing combined with stroboscopic sampling. The same refocusing scheme is also applied during the evolution period. In the simplest version, the repetitive refocusing is obtained by a Carr–Purcell–Meiboom–Gill (CPMG) pulse sequence (*18, 19*), as it has been applied in Ref. (*20*) for distance measurements in doubly ^{13}C-labeled organic compounds.

It has been recognized that pulse imperfections have a cumulative effect in the CPMG sequence, and several compensated pulse sequences have been proposed (*21–24*). Levitt and Freeman (*21*) have pointed out that the tolerance of the CPMG pulse sequence to pulse errors and resonance offset can be increased by using composite pulses. Maudsley remarked that Fourier imaging experiments could benefit from using a phase-alternated CP sequence of the type $(\tau, \pi_x, \tau, \pi_y, \tau, \pi_x, \tau, \pi_y)_n$ (*22*), later referred to as the ''xy-4'' sequence (*24*). Shaka *et al.* demonstrated (*23*) that the MLEV iteration scheme, originally introduced for deriving highly compensated windowless decoupling sequences (*25*), could also be applied to multiple π pulse sequences. Gullion *et al.* suggested (*24*) supercycled variants (xy-8, xy-16) of the xy-4 sequence and found their performance in removing inhomogeneous broadening in liquid water to be superior to that of MLEV cycles of the same length.

In order to obtain purely dipolar spectra from doubly labeled solids, it is important that the applied pulse sequence efficiently eliminates the effect of the chemical shifts even in the presence of pulse imperfections. As the chemical shift difference term does not commute with H_d, this requirement is not automatically met by pulse sequences that lead to long echo life times in liquids. Dipolar spectra of doubly ^{13}C-labeled organic compounds have been measured using the CPMG sequence at a low static field corresponding to a ^{13}C resonance frequency of 15 MHz (*20*). At higher fields, where the relative importance of chemical shift terms in the Hamiltonian is larger, dipolar spectra have been obtained using the xy-8 and xy-16 sequences (*26*) and an MLEV-4 sequence with a single π pulse as an elementary rotation (*27*), which we will refer to as ''xx-4.''

TABLE 1
Average Hamiltonian Terms of Zeroth and First Order for Different Variants of the CPMG Pulse Sequence

Name	Pulse sequence	$\bar{H}^{(0)} - H_d$	$\bar{H}^{(1)}$
CPMG	$[(\pi)_x(\pi)_x]_n$	$\xi\tau^{-1}(S_{1x} + S_{2x})$	0
xx-2	$[(\pi)_x(\pi)_{-x}]_n$	0	$\xi(\omega_{01}S_{1y} + \omega_{02}S_{2y}) + \xi b_{12}\frac{3}{2}(S_{1z}S_{2y} + S_{1y}S_{2z})$
xy-4	$[(\pi)_x(\pi)_y(\pi)_x(\pi)_y]_n$	0	$\xi b_{12}\frac{3}{4}(S_{1z}S_{2x} + S_{1x}S_{2z} + S_{1z}S_{2y} + S_{1y}S_{2z})$
xx-4	$[(\pi)_x(\pi)_x(\pi)_{-x}(\pi)_{-x}]_n$	0	0

In the following, we will compare several variants of the basic CPMG scheme in view of their sensitivity to pulse rotation angle errors based on coherent averaging theory (*28*). In particular, the efficiency in suppressing chemical shifts in the presence of strong dipolar couplings will be discussed. In order to retain formally the cyclic property of the pulse sequences, the actual rotation angle is written as $\pi - \xi$, where ξ represents a small deviation from the ideal π rotation and the error term is incorporated into the ''unperturbed'' Hamiltonian $H(t)$:

$$H(t) = \omega_{01}S_{1z} + \omega_{02}S_{2z} + H_d + \frac{\xi}{\pi}H_p(t). \qquad [10]$$

$H_p(t)$ represents the time-dependent Hamiltonian of the ideal pulse sequence. The pulses are assumed to be short and to effect instantaneous rotations in spin space (δ-function limit).

The toggling-frame Hamiltonian after the nth pulse is obtained, as usual, by a transformation by the (ideal) pulse sequence $H_p(t)$ with the individual pulse rotations P_k:

$$\bar{H}_n = P_1^{-1}P_2^{-1}\cdots P_n^{-1}H(t)P_n\cdots P_2P_1. \qquad [11]$$

Under a series of π rotations, the dipolar coupling term in the toggling frame Hamiltonian remains invariant, whereas the shift term changes sign after each pulse. This leads to the desired averaging of the chemical shifts. In the toggling frame, the pulse error term will turn into a comb of instantaneous ξ rotations.

Because the chemical shift difference term $\Delta\omega(S_{1z} - S_{2z})$ does not commute with the dipolar term H_d, all repetitive multiple π pulse refocusing sequences with pulse separation τ lead to a nonzero second-order average Hamiltonian even in the limit of ideal pulses:

$$\bar{H}^{(2)} = \frac{b_{12}^2\Delta\omega\tau^2}{64}(S_{1z} - S_{2z}) + \frac{b_{12}(\Delta\omega)^2\tau^2}{48}(S_{1x}S_{2x} + S_{1y}S_{2y}). \qquad [12]$$

For satisfactory performance, $\bar{H}^{(2)}$ must be made much smaller than H_d by using a sufficiently high pulse-repetition rate. This leads to the condition

$$\tau \ll \min\left\{\frac{8}{\sqrt{b_{12}\Delta\omega}}, \frac{4\sqrt{3}}{\Delta\omega}\right\}. \qquad [13]$$

Four different pulse sequences, which all lead to a purely dipolar average Hamiltonian in the limit of a high repetition rate and for vanishing pulse rotation angle errors, will be compared in the following. Their average Hamiltonians of zeroth and first order are given, to first order in ξ, in Table 1.

In the case of the CPMG sequence, all error terms in the toggling-frame Hamiltonian are of the same sign, and their effects thus accumulate in the zero-order average Hamiltonian, leading to an error term that diverges for short pulse separation τ. Since rapid pulse repetition is needed for proper averaging of the chemical shift terms, as explained above, it is to be expected that the CPMG sequence will perform poorly in the present context.

The accumulation of errors can be eliminated by simply alternating the sign of consecutive π pulses in the CPMG sequence. We will refer to this sequence as ''xx-2.'' Although $\bar{H}^{(0)}$ is now free of error terms, the nonsymmetric nature of the toggling-frame Hamiltonian leads to a nonvanishing first-order average Hamiltonian that reintroduces the chemical shifts.

In the case of the xy-4 sequence, which equally eliminates errors in $\bar{H}^{(0)}$, there is also a nonvanishing first-order average Hamiltonian. However, it only contains the dipolar coupling constant and thus does not reintroduce chemical shift effects. For the doubly ^{13}C-labeled bisphenol-A polycarbonate samples that have been used in this study, this represents a considerable advantage over the xx-2 sequence, since the chemical shift anisotropy is on the order of 160 ppm, which translates, in a spectrometer operating at a proton resonance frequency of 220 MHz, to more than 8 kHz, compared to a dipolar coupling constant of only 1 kHz.

The first-order average Hamiltonian can be eliminated al-

together by modifying the pulse sequence such that a symmetric toggling-frame Hamiltonian results. This can be achieved by alternating the sign of the rotations in the CPMG sequence after every *second* pulse, leading to what we term the xx-4 sequence. The xy-8 and xy-16 sequences (*24*), which are symmetrized variants of the xy-4 sequence, achieve the same result. Experimentally, the performances of the xx-4 and xy-4 sequences were found to be nearly equivalent, and both sequences are adequate in the context of the dipolar DECODER experiment (cf. Fig. 4A under Results and Discussion).

Decomposition of the Orientational Distribution Function

The procedure for retrieving the orientational information from the spectral data is analogous to that described in Ref. (*11*). In the present case, the orientation of an internuclear vector is of interest, and the analysis can be made in terms of spherical-harmonic basis functions, rather than in terms of the more general Wigner rotation-matrix elements.

The following conventions for the definition of reference frames and rotations between them will be used:

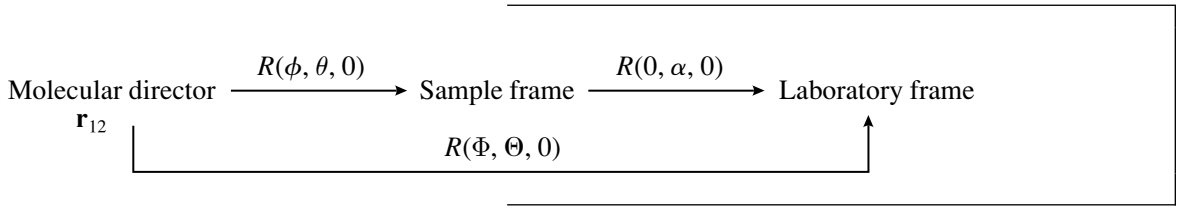

The orientational distribution of the internuclear vector $\mathbf{r}_{12}$ is described by the probability $P(\theta, \phi)\sin\theta d\theta d\phi$ of finding it at the polar angles (θ, ϕ). The orientational distribution function $P(\theta, \phi)$ can be decomposed into a sum of spherical harmonics (*29, 30*)

$$P(\theta, \phi) = \sum_{l,m} c_{lm} C_{lm}(\theta, \phi),\ l \in \{0, 2, 4, \cdots\} \times m \in \{-l, -l+1, \cdots, l\}. \quad [14]$$

The dipolar DECODER spectra $\mathsf{S}(\omega_1, \omega_2)$ can then be considered as a superposition of basis spectra $\mathsf{S}_{lm}(\omega_1, \omega_2)$, each associated with a spherical-harmonic probability-distribution basis function (*7, 11, 31*):

$$\mathsf{S}(\omega_1, \omega_2) = \sum_{l,m} c_{lm} \mathsf{S}_{lm}(\omega_1, \omega_2). \quad [15]$$

In order to retrieve the orientational information, contained in the coefficients c_{lm}, from the experimental spectrum $\mathsf{S}(\omega_1, \omega_2)$, the above relationship must be inverted. This can be achieved by calculating the integrals of the products of the experimental spectrum with the basis spectra, yielding the coefficients

$$a_{lm} = \int_{\omega_1} \int_{\omega_2} \mathsf{S}(\omega_1, \omega_2) \mathsf{S}_{lm}(\omega_1, \omega_2) d\omega_1 d\omega_2. \quad [16]$$

These coefficients must be converted into the expansion coefficients c_{lm} by inversion of the linear relationship (*11*)

$$a_{lm} = \sum_{l',m'} c_{l'm'} \underbrace{\int_{\omega_1} \int_{\omega_2} \mathsf{S}_{l'm'} \mathsf{S}_{lm} d\omega_1 d\omega_2}_{G_{l'm'lm}}. \quad [17]$$

The order parameters $\langle C_{lm} \rangle$ are then

$$\langle C_{lm} \rangle = \frac{c_{lm}}{2l+1}. \quad [18]$$

It can occur that the matrix $G_{l'm'lm}$ is singular, reflecting the fact that the basis spectra are not independent and the measurement is insufficient for their separation. In this case, the basis must be reduced to a subset that is fully determined. In addition, *a priori* knowledge about the symmetry of the orientational distribution leads to constraints for the expansion coefficients c_{lm}. The orientational distribution resulting from a deformation process must reflect the symmetry of the deformation mode. In particular, the plane strain deformation that is under study here leads to D_{2h} symmetry of the sample. Together with the invariance of the dipolar interaction tensor upon point inversion and the fact that the orientational distribution function is real, this leads to the constraints

$$c_{lm} = 0 \quad \text{for } l \text{ or } m \text{ odd};$$
$$c_{lm} = c_{l,-m}. \quad [19]$$

For lower symmetry of the sample, which could for instance result from an inhomogeneous deformation, also basis functions with even l, but odd m must be included into the analysis.

As has been pointed out by Schmidt-Rohr *et al.* (*8*), it

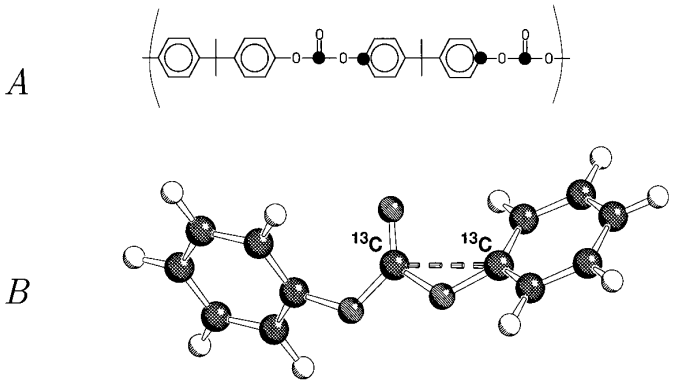

FIG. 2. (A) Repeating unit of bisphenol-A polycarbonate. The marked atoms are isotopically enriched to 99% ^{13}C. (B) Ball and stick plot of diphenyl-carbonate, showing the preferred geometric arrangement around the labeled site. The orientational distribution of the internuclear vector marked as a dashed bond is measured.

is possible to extract the orientational distribution function directly from the spectra, without any fitting procedure, provided that the interaction tensor is axially symmetric. The reason for this lies in the fact that the relationship between the orientation of the uniaxial interaction tensor and the transition frequencies can be readily inverted. Unfortunately, a complication arises in the case of dipolar DECODER spectra. Each two-spin system gives rise to *two* transitions, which leads to a spectrum symmetric with respect to point inversion at the origin. By consequence, there is a region in the two-dimensional spectral pattern where each point obtains contributions from two different orientations of the interaction tensor. In this region, direct calculation of the orientational distribution function is ambigous. Therefore, least-squares fitting by an inversion of the matrix $G_{l'm'lm}$ is preferred for the analysis of dipolar DECODER data.

EXPERIMENTAL

The sample bisphenol-A polycarbonate, specifically enriched with ^{13}C at the carbonate unit and at the phenylene unit (Fig. 2), has been selected in the context of a more extended series of studies (*14*) devoted to the investigation of torsional-angle distribution functions in polycarbonate. With this particular pair of labeling sites, it is possible to quantify the angular distribution within the carbonyl-phenyl moiety. In view of an extension of this type of studies to deformed samples, it is, however, prerequisite to determine the orientational distribution function of the internuclear vector between all labeled sites.

Twenty percent by weight of the labeled material and 80% of natural abundance polycarbonate were dissolved together in dichloromethane to give a 2% solution by weight. The polymer was then precipitated by slowly casting the solution into the 10-fold volume of dry, cold methanol. After suction filtration, the material was dried at 60°C under vacuum (<10 mbar) for 24 h. The molecular weight of the isotopically enriched material was M_w = 36,200 and the polydispersity M_w/M_n = 1.5 (*14*). The natural abundance material used for dilution was obtained from Bayer AG (Leverkusen, Germany), and was characterized as M_w = 34,270, M_w/M_n = 2.2. It was used without further purification. Dense, rectangular samples of 5 mm height, 5 mm width, and 10 mm length were obtained by compression of the material in a rectangular die under a uniaxial load of 2 GPa at 250°C during 2 min. The samples were then slowly (>100 min) cooled to room temperature. Inspection of the dense samples under polarized light showed no trace of inhomogeneity.

The plane-strain deformation was executed in a homebuilt channel-die setup (cf Fig. 3A) at 300 K. Friction between the sample and the walls of the die was reduced by means of a perfluorinated lubricant. The channel die was fitted to a mechanical testing machine that was programmed such

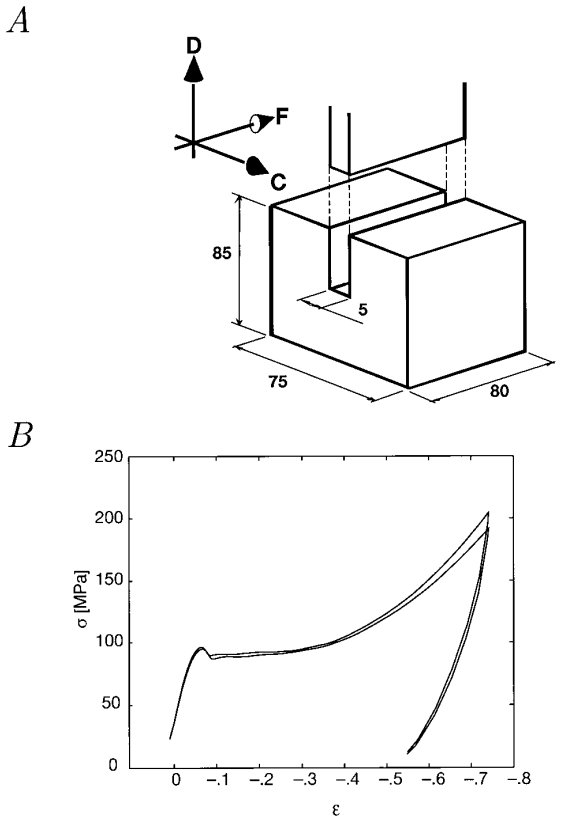

FIG. 3. (A) Sketch of the channel-die apparatus that has been used for the deformation experiment. Dimensions are in millimeters. The compression stamp is moved along the deformation direction D. The flow of the sample is constrained by the rigid walls of the die in the direction C, and free flow is possible in the direction F. (B) Stress (σ)–strain (ϵ) diagram resulting from channel-die extrusion of bisphenol-A polycarbonate at 300 K and a strain rate of $\dot{\epsilon}$ = 0.01 s^{-1}.

that the remaining separation between the die and the stamp followed an exponential decay. This leads to a constant strain rate $\dot{\varepsilon} = (d/dt)\ln(l/l_0)$. Two samples were deformed up to a maximum strain of $\varepsilon = \ln(l/l_0) = -0.75$. The deformation rate was $\dot{\varepsilon} = -0.01\ s^{-1}$ in both cases. The strain data from the deformation experiments were corrected for the finite compliance of the testing machine.

The NMR measurements were conducted on a homebuilt spectrometer operating at a proton resonance frequency of 220 MHz. The pulse sequence shown in Fig. 1 was used in this study. The RF field strength was adjusted to 40 kHz for Hartmann–Hahn cross polarization and for *I*-spin decoupling, and to 96 kHz for short RF pulses. The Hartmann–Hahn contact time was 2 ms in all cases. In order to avoid unwanted cross polarization, the decoupling was suspended during the refocusing pulses, as shown in Fig. 1.

A homebuilt probe assembly allows the sample to be rotated or flipped under the control of the spectrometer computer by means of a DC motor mounted outside the bore of the magnet and a bevel gearing inside the thermally insulated sample chamber. The orientation of the sample is monitored by an optical coding disk at a resolution of 1024 steps per full revolution. The position is continuously fed back into a programmable control unit which is connected to the spectrometer computer. At the beginning of the flip delay, the sample was accelerated at a rate of 100 rad s^{-2} up to a maximum angular velocity of 50 rad s^{-1}, and then decelerated at the same rate. A time of 80 ms is needed for the completion of a 90° flip. Nevertheless, the flip delay was set to 200 ms to allow for the decay of any mechanical vibrations the sample flip might have caused. It was demonstrated by recording two-dimensional spectra at zero flip angle that there is no detectable spin-diffusion contribution during the 200 ms.

One-dimensional spectra were recorded at 135 and 300 K. The temperature for the two-dimensional spectra was set to 300 K.

RESULTS AND DISCUSSION

Deformation

The stress–strain diagram recorded during the channel-die extrusion experiment, used to deform the sample, is given in Fig. 3B. After a period of elastic loading, there is a clear yield point at a stress σ of about 100 MPa, followed by smooth plastic flow up to a deformation of $\varepsilon = -0.4$. At that point, the resistance of the material to further deformation starts to increase. The two curves in Fig. 3B correspond to two experiments on different samples, demonstrating the satisfactory reproducibility. The observed stress–strain curves are quantitatively in good agreement with the results reported by Arruda and Boyce (*32*).

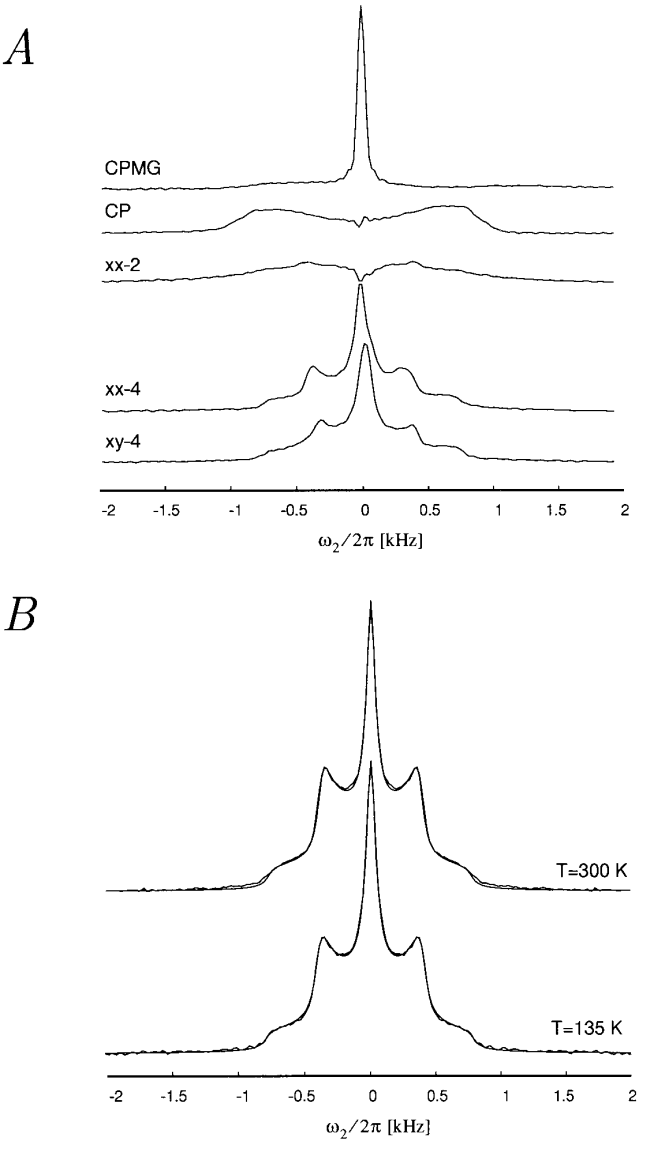

FIG. 4. (A) Dipolar spectra of undeformed doubly ^{13}C-labeled bisphenol-A polycarbonate recorded at 300 K using different refocusing pulse sequences as indicated in the figure. (B) One-dimensional symmetrized dipolar spectra of undeformed doubly ^{13}C-labeled bisphenol-A polycarbonate recorded using the xy-4 sequence at 300 K (upper trace) and at 135 K (lower trace). The spectra are fitted by a theoretical Pake lineshape plus a central delta function, broadened by a Lorentzian function. The dipolar splitting is found to be 5% larger at 135 K than at room temperature. The quality of the fit demonstrates the performance of the xy-4 sequence in suppressing chemical shifts.

1D Spectra

One-dimensional spectra of undeformed doubly ^{13}C-labeled bisphenol-A polycarbonate have been recorded using different refocusing sequences in order to evaluate their efficiency in suppressing chemical shifts. The results are given in Fig. 4A. The duration of the π pulses has been

adjusted such as to maximize the sharpness of the pattern resulting from the xy-4 sequence, and then reduced by 5% for the measurement of the spectra in Fig. 4A, in order to emphasize the performance in the presence of pulse rotation angle errors.

For the CPMG sequence, a single peak at zero frequency is observed, superimposed on a broad pattern that is almost lost in the noise. The central peak can be attributed to isolated natural abundance ^{13}C nuclei, for which the CPMG refocusing scheme is expected to be rather effective. Indeed, if the phase of the π pulses is rotated by 90° with respect to the initial cross-polarization step (CP sequence), the central peak is lost due to rapid dephasing under the pulse rotation angle errors. Probably both the isolated natural abundance ^{13}C nuclei and those in the doubly labeled monomeric units contribute to the broad pattern that is observed.

The phase-alternated sequence xx-2 produces a pattern that bears some resemblance to a Pake doublet. No central peak is observed because of the first-order average Hamiltonian, which contains, even for isolated spins, an error term of the type $\xi\omega_{0j}S_{jy}$.

The xx-4 and xy-4 sequences produce both a slightly asymmetric Pake doublet together with a sharp central peak. The spectral asymmetry can be reduced substantially for both sequences by proper adjustment of the pulse length.

Using the xy-4 sequence with optimized π pulses, one-dimensional dipolar spectra recorded at 300 K and 135 K are given in Fig. 4B. A theoretical Pake lineshape and a central δ function, convoluted with a Lorentzian broadening function, have been used to fit the experimental spectra; the coupling constant

$$d_{12} = \frac{\mu_0}{4\pi}\frac{\gamma_s^2\hbar}{r_{12}^3},$$

the height of the central delta peak, and the width of the Lorentzian are the free parameters of the fit. The coupling constants determined from the two spectra are $d_{12}/2\pi = 800 \pm 10$ Hz at 135 K and $d_{12}/2\pi = 764 \pm 15$ Hz at 300 K. The quality of the fit is very good for both temperatures, albeit small deviations from the ideal lineshape are manifest at the base of the central peak and in the wings of the Pake doublet at 300 K. The lower quality of fit and the slightly lower coupling constant that are observed at 300 K can be explained in terms of small-amplitude motions of the internuclear vector, which are present at room temperature but frozen out at 135 K.

The quality of the fit verifies the efficiency of the xy-4 sequence. Due to the large anisotropy of the chemical shift tensors for both the carbonate and the phenylene carbon, which is an order of magnitude larger than the dipolar coupling constant, imperfect suppression of the chemical shift term would lead to substantial broadening and to deviations from the ideal powder lineshape.

It has been demonstrated that the observed splitting in dipolar spectra, acquired under multiple pulse refocusing of the chemical shifts, is scaled linearly with $1 - D$, where D represents the duty factor $D = t_w/\tau$, t_w being the duration of the π pulses (*20, 33*). In the experiments reported here, the duty factor was always below 12%. Within experimental error, no change in the apparent dipolar coupling constant could be observed upon variation of the duty factor from 5 to 10%. However, as the dipolar DECODER experiment is not intended for measuring internuclear distances, the absolute value of the dipolar coupling is not of great importance in this context.

2D Spectra

The two-dimensional spectra shown in Fig. 5 have been recorded with the pulse sequence of Fig. 1. They have been symmetrized with respect to point inversion at the origin because of the C_2 symmetry of the theoretical patterns. Deviations from exact symmetry evident in Fig. 5 are due to the contour drawing routine that has been used.

The sample was flipped by an angle of $\alpha = 90°$. During t_1, the deformation direction D was parallel to the static magnetic field while during t_2 the constrained direction C was rotated into this direction. The selection of a 90° sample flip leads, in general, to a loss of information in DECODER spectra (*8*). Instead of sampling the distribution function in a full quadrant of the unit sphere, only an octant is significant in this case, the remainder related by symmetry, and it has been shown that the spectral area available for the reconstruction of the orientational distribution is largest at $\alpha = 45°$ (*8*). For the present study, however, this is of no consequence, as a deformation mode that leads to D_{2h} symmetry of the sample has been used.

A 90° sample flip leads to a triangular ridge pattern as the basic building unit of the spectra, each corner of which corresponds to internuclear vectors aligned with one of the three specific directions of the sample as indicated in Fig. 5. Due to symmetry, the triangular ridge is replicated, leading to the characteristic peak shape reminiscent of a deformed six-cornered star. As in the one-dimensional spectra, the presence of isolated natural-abundance ^{13}C nuclei in the sample leads to a sharp central peak.

In the case of the undeformed sample, the isotropy of the orientational distribution is reflected in the symmetry of the observed spectral pattern with respect to the antidiagonal.

The anisotropy of the deformed sample is revealed by taking the difference between the deformed and undeformed spectra in Fig. 5. Whereas there is excess intensity in the region corresponding to the free direction, the intensity is reduced at the two other corners in the spectrum of the

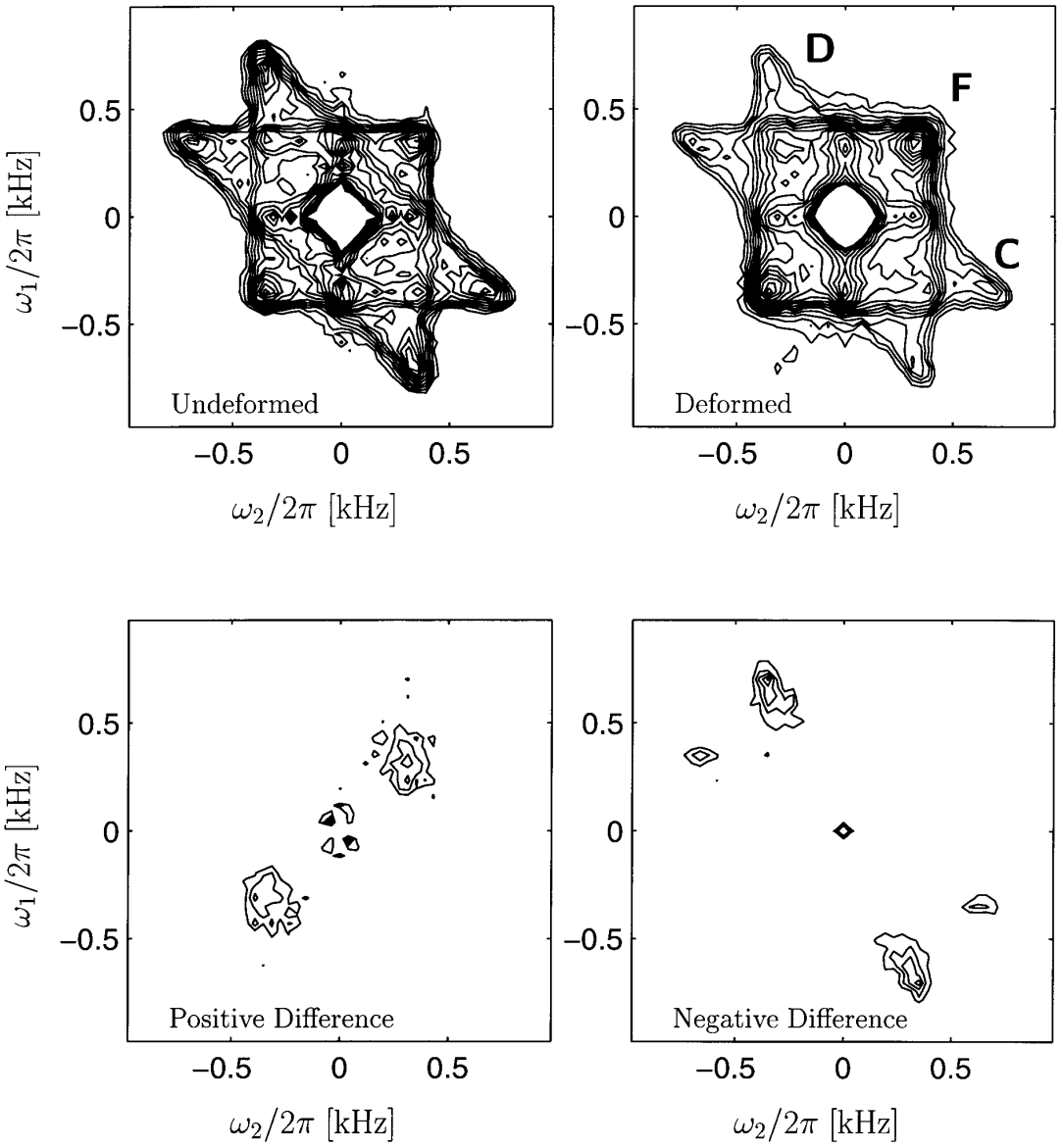

FIG. 5. Dipolar DECODER spectra of ^{13}C-labeled bisphenol-A polycarbonate before and after deformation. The spectra exhibit a characteristic star-like ridge pattern. Each of the three types of corners (*C*, *D*, *F*) in the pattern corresponds to vectors oriented along a particular direction in the channel-die of Fig. 3A, as indicated. The anisotropy that is caused by the deformation becomes readily visible in the difference spectrum (deformed–undeformed, bottom). For clarity, the negative (right) and positive contours (left) have been drawn separately.

deformed sample. The depletion is more pronounced for the deformation direction than for the constrained direction. The possibility of deriving qualitative data about the orientational distribution just by visual inspection of dipolar DECODER spectra is an advantage of the method. In order to retrieve quantitative information from the spectra, they were decomposed into a set of basis spectra, corresponding to the spherical-harmonic basis functions of the orientational distribution function, as outlined above. The analysis was carried out for basis functions up to order 4. The matrix *G* (see above) was found to have full rank; hence, the order parameters are fully determined by the dipolar DECODER spectrum.

The basis spectra were calculated in the δ-function limit using the dipolar coupling constant that had resulted from the fit of the one-dimensional spectra. A central δ peak was added to the isotropic basis spectrum S_{00}, and all basis spectra were convoluted with a Lorentzian broadening function. The height of the central peak and the width of the broadening function were determined from a least-squares fit to the spectrum of the sample before deformation.

TABLE 2
Order Parameters Determined from Decomposition of Measured Spectra

Order parameter	Before deformation	After deformation
$\langle C_{0,0}\rangle$	1.0000	1.0000
$\langle C_{2,0}\rangle$	0.0034 ± 0.0071	−0.0174 ± 0.0050
$\langle C_{2,2}\rangle$	−0.0003 ± 0.0017	−0.0094 ± 0.0012
$\langle C_{4,0}\rangle$	−0.0003 ± 0.0027	−0.0083 ± 0.0019
$\langle C_{4,2}\rangle$	0.0014 ± 0.0058	0.0029 ± 0.0042
$\langle C_{4,4}\rangle$	0.0033 ± 0.0047	0.0043 ± 0.0033

The order parameters that resulted from the decomposition are compiled in Table 2. The error margins represent deviations resulting in an increase of the mean square residual of fit by twice the variance of amplitude in the spectral regions that contain vanishing signal. The orientational distributions reconstructed from the order parameters are given in Fig. 6 in the form of polar diagrams. The probability density (normalized such that it is 1 for an isotropic distribution) is plotted as a function of the polar angles θ (radius) and ϕ (azimuth). The upper graph in Fig. 6, recorded before deformation, shows only minor deviations from uniformity which have their origins in small measurement errors, thus giving an indication of the lower limit of the orientational sensitivity of the method.

In the lower graph in Fig. 6, the anisotropy resulting from the channel-die extrusion is clearly visible. As was already apparent qualitatively from the difference spectra in Fig. 5, the probability density is highest in the region corresponding to alignment of the internuclear vector with the free direction in the channel die, whereas there is pronounced depletion along the deformation direction. Along the constrained direction, the probability density is very close to 1. The orientational distribution thus reflects the planar mode of deformation that results from the channel-die experiment. The magnitude of the order parameters is in the same range as what has been found for similar strains in uniaxial compression (*11*). An interpretation of the measured data in terms of constitutive models for polycarbonate, such as those developed by Arruda and Boyce (*32*), or in terms of atomistic simulations (*34*) is possible. However, it requires a systematic investigation of the orientational order as a function of deformation. Such work is currently in progress and will be reported later.

CONCLUSIONS

It has been found that the dipolar DECODER experiment is a useful addition to the existing techniques for the quantitative measurement of orientational distribution functions in macroscopically anisotropic samples as they arise in deformation experiments. The required purely dipolar spectra can be obtained conveniently by a multiple-pulse chemical shift refocusing experiment using the xy-4 or equivalently the xx-4 sequences which are remarkably insensitive to pulse flip-angle errors. An obvious prerequisite of the dipolar DE-

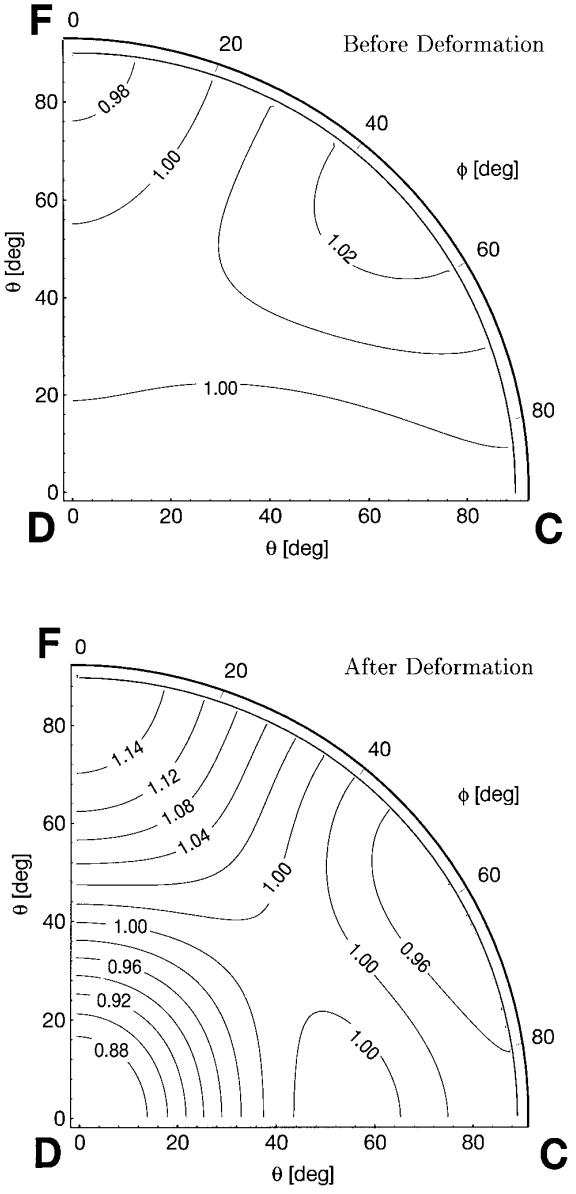

FIG. 6. Polar diagrams as functions of θ and ϕ of the orientational distributions as determined from the dipolar DECODER spectra measured before (top) and after deformation (bottom). The distribution is nearly uniform before the deformation, whereas there is clear enrichment of labeled internuclear vectors aligned with the free direction of the channel die, and corresponding depletion around the deformation direction, in the case of the deformed sample. The orientations *C*, *D*, and *F* correspond to those in Fig. 3A.

CODER experiment is the availability of a doubly labeled sample. In many situations such samples must be prepared for other reasons, for example, for the study of torsional angle distribution functions (*14*). Then, the application of the dipolar DECODER experiment can be the preferred technique for the study of orientational anisotropy. It has recently been demonstrated that the acquisition of purely dipolar spectra using multiple-pulse refocusing of chemical shifts is also possible for heteronuclear two-spin systems (*33*). Thus, heteronuclear variants of the dipolar DECODER experiment, for instance using $^{13}C-^{15}N$ doubly labeled samples, are also conceivable.

The dipolar DECODER technique is to be compared with the quadrupolar DECODER experiment that requires selective deuterium labeling. Often the very large spectral range of deuterium quadrupolar spectra leads to experimental problems in the context of 2D spectroscopy. Such difficulties are nonexistent for the dipolar DECODER technique with spectra of convenient width. A significant advantage of the dipolar interaction tensor is its rotational symmetry which leads to simpler peak shapes and facilitates the interpretation and fitting of the resulting 2D spectra. This advantage becomes particularly apparent when comparing with a CSA–DECODER experiment where asymmetry is usually significant. On the other hand, the orientational information that is available by using an asymmetric reporter tensor is greater, provided it can be fully exploited.

ACKNOWLEDGMENTS

We gratefully acknowledge valuable support in performing the mechanical testing experiments by Ludger Weber, Reliability Laboratories, ETH Zürich, as well as essential discussions with Dr. Marco Tomaselli and excellent technical support from Paul Signer. This work has been supported by the Swiss National Science Foundation.

REFERENCES

1. I. M. Ward, ''Mechanical Properties of Solid Polymers,'' Wiley–Interscience, London (1971).
2. L. Monnerie, *in* ''Developments in Oriented Polymers'' (I. M. Ward, Ed.), Vol. 2, Elsevier, Amsterdam (1987).
3. L. E. Alexander, ''X-Ray Diffraction Methods in Polymer Science,'' Wiley–Interscience, New York (1969).
4. F. J. Baltá-Calleja and C. G. Vonk, ''X-Ray Scattering of Synthetic Polymers,'' Elsevier, Amsterdam (1989).
5. M. Pick, R. Lovell, and A. H. Windle, *Polymer* **21,** 1017 (1980).
6. P. M. Henrichs, *Macromolecules* **20,** 2099 (1987).
7. G. S. Harbison, V.-D. Vogt, and H. W. Spiess, *J. Chem. Phys.* **86,** 1206 (1987).
8. K. Schmidt-Rohr, M. Hehn, D. Schaefer, and H. W. Spiess, *J. Chem. Phys.* **97,** 2247 (1992).
9. B. F. Chmelka, K. Schmidt-Rohr, and H. W. Spiess, *Macromolecules* **26,** 2282 (1993).
10. R. H. Lewis, H. W. Long, K. Schmidt-Rohr, and H. W. Spiess, *J. Magn. Reson. A* **115,** 26 (1995).
11. M. Utz, M. Tomaselli, R. R. Ernst, and U. W. Suter, *Macromolecules* **29,** 2909 (1996).
12. C. Griesinger, O. W. Sørensen, and R. R. Ernst, *J. Chem. Phys.* **85,** 6837 (1986).
13. C. Schmidt, B. Blümich, and H. W. Spiess, *J. Magn. Reson.* **79,** 269 (1988).
14. M. Tomaselli, P. Robyr, B. Meier, C. Grob-Pisano, R. R. Ernst, and U. W. Suter, *Mol. Phys.* **89,** 1663 (1996).
15. A. Kumar and R. R. Ernst, *J. Magn. Reson.* **24,** 425 (1976).
16. A. Kumar, *J. Magn. Reson.* **30,** 227 (1978).
17. G. Bodenhausen, R. Freeman, G. A. Morris, and D. L. Turner, *J. Magn. Reson.* **31,** 75 (1978).
18. H. Y. Carr and E. M. Purcell, *Phys. Rev.* **94,** 630 (1954).
19. S. Meiboom and D. Gill, *Rev. Sci. Instrum.* **29,** 688 (1958).
20. M. Engelsberg and C. S. Yannoni, *J. Magn. Reson.* **88,** 393 (1990).
21. M. H. Levitt and R. Freeman, *J. Magn. Reson.* **43,** 65 (1981).
22. A. A. Maudsley, *J. Magn. Reson.* **69,** 488 (1986).
23. A. J. Shaka, S. P. Rucker, and A. Pines, *J. Magn. Reson.* **77,** 606 (1988).
24. T. Gullion, D. B. Baker, and M. S. Conradi, *J. Magn. Reson.* **89,** 479 (1990).
25. M. H. Levitt, R. Freeman, and T. Frenkiel, *in* ''Advances in Magnetic Resonance'' (J. S. Waugh, Ed.), pp. 47–110, Academic Press, New York (1983).
26. M. J. Lizak, T. Gullion, and M. S. Conradi, *J. Magn. Reson.* **91,** 254 (1991).
27. D. P. Weliky, G. Dabbagh, and R. Tycko, *J. Magn. Reson. A* **104,** 10 (1993).
28. U. Haeberlen, ''High Resolution NMR in Solids—Selective Averaging,'' Supplement 1 to Advances in Magnetic Resonance, Academic Press, New York (1976).
29. R.-J. Roe and W. Krigbaum, *J. Chem. Phys.* **40,** 2608 (1964).
30. V. J. McBrierty, *J. Chem. Phys.* **61,** 872 (1974).
31. R. Hentschel, J. Schlitter, H. Sillescu, and H. Spiess, *J. Chem. Phys.* **68,** 56 (1978).
32. E. M. Arruda and M. C. Boyce, *Int. J. Plast.* **9,** 697 (1993).
33. Y. Ishii and T. Terao, *J. Magn. Reson. A* **115,** 116 (1995).
34. M. Hutnik, A. Argon, and U. Suter, *Macromolecules* **26,** 1097 (1993).